



DYNAMIC TESTING OF PROTOTYPE PRESSURE CONTROLLED AIR DAMPER UNDER CYCLIC LOADING PROTOCOL

Utsav K. Koshti

Research Scholar, Department of Civil Engineering,
Institute of Technology, Nirma University, Ahmedabad, Gujarat, India

Sharadkumar Purohit

Professor, Department of Civil Engineering, School of Engineering,
Institute of Technology, Nirma University, Ahmedabad, Gujarat, India

ABSTRACT

Passive damping devices can effectively control the seismic structural response of the building in which they are fitted. The paper aims to develop a prototype Pneumatic Controlled Air Damper (PCAD) and study its hysteresis behaviour under cyclic displacement input under varying frequencies. A piston based pneumatic cylinder was used to fill with air under external pressure of 1.0 bar and 1.5 bar. The prototype PCAD device, so developed, exhibits elliptical shaped stable hysteresis loop under each displacement input frequency ensuring energy dissipation capabilities. The damper force produced by the PCAD increases with each frequency of displacement input as well as with the increase in the external pressure applied. The PCAD shows energy dissipation characteristics, measured by an equivalent viscous damping coefficient, ζ , improves with input motion frequencies but found to decrease with an increase in the external pressure. The PCAD works efficiently for low frequencies of displacement input.

Keywords: Air Damper, Shake Table, Hysteresis Loop, Damping Coefficient

Cite this Article: Utsav K. Koshti and Sharadkumar Purohit, Dynamic Testing of Prototype Pressure Controlled Air Damper Under Cyclic Loading Protocol, International Journal of Civil Engineering and Technology (IJCIET), 15(2), 2024, pp. 1-12.

<https://iaeme.com/Home/issue/IJCIET?Volume=15&Issue=2>

1. INTRODUCTION

Increased seismic events, worldwide, in the recent past offer a stiff challenge to the structural engineering fraternity for controlling earthquake resistant buildings. It has been realized that earthquake occurrences, cause widespread damage to manmade structures and lifeline structures and take millions of human lives. In countries like India, which are still developing, a large part of the land is at risk of strong earthquakes. Many buildings are vulnerable, and even so, there's a big demand for new construction projects [1]. It is imperative to build earthquake resistant buildings and/or mitigate the risk of seismic damage to existing buildings. Various means of controlling seismic damage to the buildings were developed over a period of time, and out of these seismic structural response control using supplemental damping to the structure becomes feasible and workable technology.

The main goal of structural response control is to prevent resonance, large amplitude oscillations, unstable vibrations, and transient vibrations. As a result of structural response control research, many damping systems have been developed using different technologies [2]. Many researchers have studied different types of structural response control systems to enhance the seismic load-resisting capabilities of the structures. The control of structural vibrations produced by earthquakes can be done by various means, such as modifying rigidities, masses, damping, or shape, and by providing passive or active counterforces [3]. For over years, researchers have been investigating the prospect of adopting active, hybrid, and semi-active control methods to improve control of structure in comparison to passive control methods. These methods include active control, hybrid control, and semiactive control, and lots of research has been conducted in the past twenty years [4], [5]. However, research interest in the development of passive damping devices is not diminishing due to the robustness and ease of installation to such devices. Research efforts have been continued to improve existing passive damping devices alongside innovations in there devices through other forms of materials with viscoelastic properties.

Passive control devices have effectively been implemented with mid-height to high-rise buildings to reduce the impact of wind excitation and earthquakes by absorbing energy through various mediums. These devices include Viscous Fluid Damper, Friction Damper, Metallic Damper and Viscoelastic Damper devices that provide vibration control and energy dissipation while being easy to install in buildings [6]. Seismic structural response control of buildings equipped with passive damping devices is now a well-established solution to mitigate their seismic vulnerability. Additionally, these devices were found equally effective against other forms of transient loading like impact and shock loading. Characteristics associated with passive energy dissipation devices, ranging from basic principles to implementational issues and design, have been addressed, and their performance was found to be excellent in a wide range of vibration structural control [7], [8].

It has been learnt that pneumatic cylinders are crucial components in various applications, such as industrial automation, robotics, and medical devices [9]. These can serve as effective damping devices in building applications, offering adjustable damping properties to attenuate the vibration response of systems. It has been seen that advancements in sensor technology, actuators, and smart materials have led to the development of more efficient, controllable pneumatic dampers for shock absorption in various mechanical applications. Pneumatic cylinders can effectively function as damping devices and vibration isolation systems for machines [10], [11]. Additionally, pneumatic suspensions, despite concerns about amplitude-dependent damping, have been utilized for vibration isolation, as evident from their experimental characterizations [12]. The application of a pneumatic cylinder as an active-controlled system for shock or vibration control was explored for the mechanical system.

However, a pneumatic cylinder as an active-controlled strategy for seismic structural response control of buildings is a new concept and has not yet been explored. Therefore, there is potential to develop a passive control pneumatic cylinder device that passively controls the seismic structural response of the building when implemented.

Few attempts have been made for the use of pneumatic and hydraulic based cylinders as passive control strategies for seismic response control. Furthermore, the assessment of hydraulic bottle jacks as effective devices for vibration control in mechanical and structural systems emphasizes the functionality of cylinder based damping devices [13]. In building applications, the damping characteristics of pneumatic cylinders can be adjusted dynamically by regulating the pressurization level within the cylinder [14]. Characterization of a prototype Vacuum-Packed Particle (VPP) damper made from polypropylene granular material under vacuum conditions was conducted under cyclic loading and with different pressure conditions ranging from 0.01MPa to 0.09 MPa to introduce the concept of a controllable VPP linear damper [15].

The present paper aims to develop a prototype Pressure Controlled Air Damper (PCAD) comprising of a pneumatic cylinder, which is low-cost and easy to install. The hysteresis behaviour of the damper is studied under cyclic displacement loading protocol of varied frequencies. Variations of the damper force with input displacement and velocity are studied to characterize the prototype damper, PCAD. The damping characterization of the prototype damper is established by evaluating energy dissipation capabilities represented by the equivalent viscous damping coefficient, ζ .

2. PROTOTYPE PRESSURE CONTROLLED AIR DAMPER

A piston-based cylinder made from aluminium casting, commercially available under the product name Janatics Pneumatic Cylinder (Model No. A120502000) was procured. The cylinder has an accumulator at one end and consists of two inlet valves, one at each end of the cylinder, which works on the principle of pressure-suction on piston movement in a forward-backward direction. A schematic diagram of the Janatics Pneumatic Cylinder is shown in Fig. 1, covering the basic details of the device.

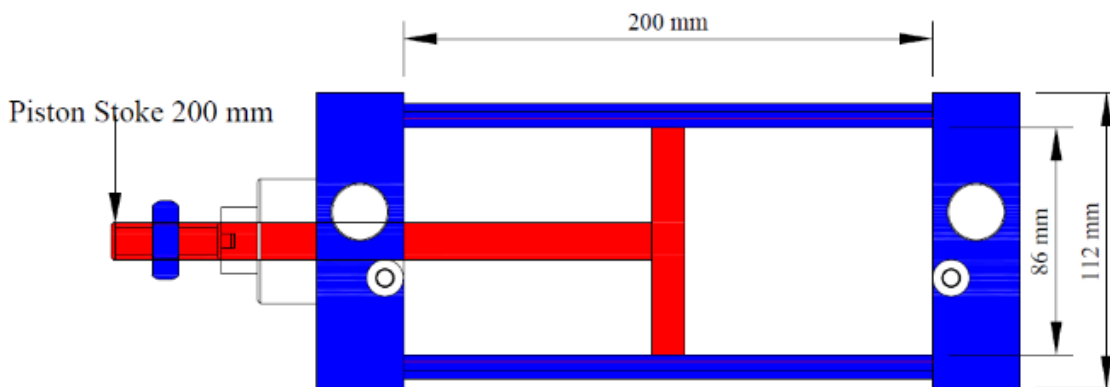


Figure 1 Schematic Diagram of Piston based Pneumatic Cylinder

It was decided to use the pneumatic damper with atmospheric pressure in its natural state, infusing external pressure through input valves at each end of the cylinder where the mean position of the piston creates two air chambers on each side of the piston. The external pressure applied to the pneumatic cylinder was controlled by an air compressor working on electric power and capable of producing air pressure up to 9.0 bar. The prototype PCAD device was subjected to external pressure of 1.0 bar and 1.5 bar to study its damping characteristics.

It was tested under cyclic displacement loading protocol with varied frequencies. The detailed workflow of the experimental programme is outlined in Fig. 2.

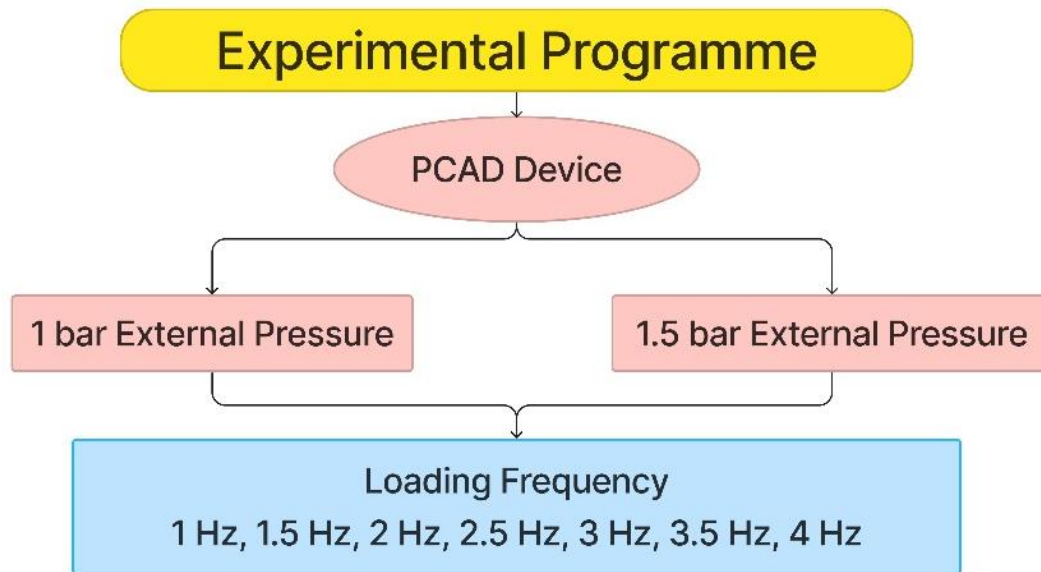


Figure 2 Details of Experimental Programme for Characterization of the Prototype PCAD

3. EXPERIMENTAL TEST SET-UP

An electrically operated and PCB-controlled small-scale shake table driven with a cam-shaft was used to perform dynamic testing of the prototype PCAD. Two shake tables available with the structural dynamics laboratory were utilized in the characterization study. One shake table platform was used to act as an inertial frame for the damper, while the other shake table was providing cyclic dynamic loading to the piston rod of the PCAD device. A few specialized assemblies were fabricated to connect the piston rod with a linearly translating shake table platform to apply controlled displacement input with varying frequencies as well as to offer a reaction at the opposite end of the pneumatic damper. A schematic diagram showing details of specialized assemblies in plan and in elevation is depicted in Fig. 3. An exhaustive instrumental programme was developed for the measurement of physical quantities of the force, acceleration, displacement and velocity of the PCAD device under varied cyclic displacement loading protocol. Sophisticated sensors, dynamic force sensors, accelerometer and linear variable differential transformer (LVDT) were employed at appropriate locations of the PCAD. A real-time measurement of force acceleration and displacement was carried out by attaching sensors with a data acquisition system from National Instruments (NI) and a high-end Computer System installed with LabVIEW software for processing and display of data in graphical output. Filter-Regulator-Lubricator (FRL) system was connected to the air compressor for ensuring controlled and good quality air to the prototype PCAD device. Fig. 3 depicts a complete experimental set-up with instrumentation used for the characterization of the prototype PCAD device under cyclic loading. A real-time photograph of the experimental set-up developed and used throughout the dynamic testing is shown in Fig. 4.

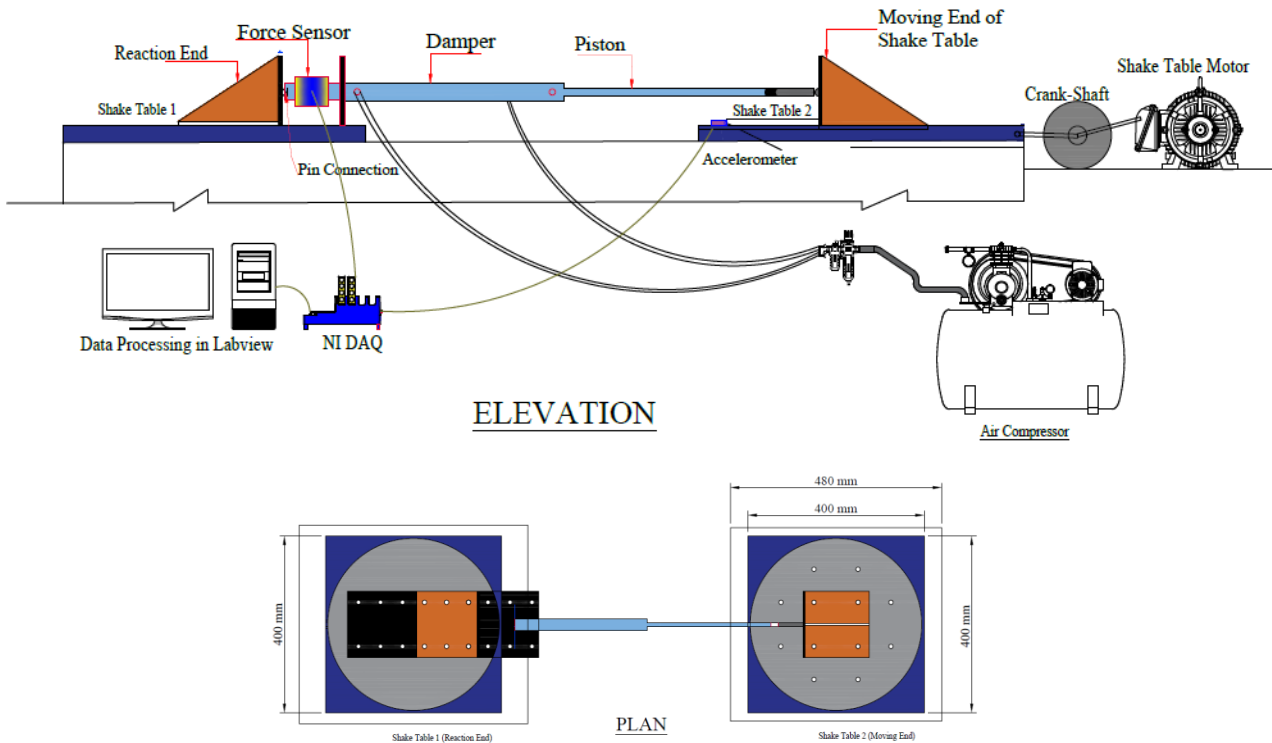


Figure 3 Schematic Diagram of Experimental Set-up with Instrumentation for Dynamic Testing of the Prototype PCAD Device

The experimental process for the air damper with external air pressure followed a similar procedure as the standard air damper test. However, an additional step was included to introduce external air pressure using an air compressor. Filter-Regulator-Lubricator (FRL) units were incorporated to regulate and maintain constant pressure. Throughout the experiment, this setup allowed for precise control of the applied air pressure. The piston movement is difficult after applying external air pressure in comparison with the air damper movement. As a result, more force value is generated. The following diagram illustrates the workflow for the experiment.



Figure 4 Real-time Photograph of Dynamic Testing of the Prototype PCAD Device through Shake Table Facility

4. RESULT AND DISCUSSION

The series of dynamic tests were initiated for PCAD with constant external 1.0 bar for varying frequencies of cyclic displacement loading applied through a shake table connected with the piston end. Real-time data of input acceleration applied to the piston end, which was integrated twice to determine the input displacement of the shake table, were captured. Simultaneously, data for the dynamic force generated by the PCAD to displacement input of applied frequency were measured. Fig. 5 (a) shows damper force plotted against input displacement for various frequencies under constant external pressure of 1.0 bar. It is evident from Fig. 5 (a) that PCAD exhibits an elliptical shaped hysteresis loop, stable over frequencies conducted for the study. It can be realized that with the increase in the frequency, the width of the hysteresis loop grows, indicating improvement in damping characteristics since it indicates better energy dissipation capabilities of the PCAD. Elliptical shaped hysteresis loops at an inclination with a horizontal axis prove that PCAD depends on the displacement of the device as it offers stiffness. It can be observed that stiffness offered by the PCAD is relatively higher for lower frequencies like 1 Hz, while stiffness tends to increase but stabilized for higher frequencies. In order to assess whether the damper force produced by PCAD depends on the velocity of the piston or not, the force-velocity relationship was plotted alongside the force-displacement relationship. A stable hysteresis loop observed for force force-velocity relationship proves that damper force is a function of piston velocity, as shown in Fig. 5 (b) for PCAD subjected to constant external pressure of 1.0 bar. A similar observation can be made when the PCAD device was subjected to constant external pressure of 1.5 bar, and force-displacement and force-velocity relationship were plotted in Fig. 6 (a) and Fig. 6 (b). It can be seen from Fig. 6 (a) that with an increase in external pressure to PCAD, stiffness offered by the damper increases substantially for a lower input frequency of 1 Hz, followed by reduced stiffness but stable hysteresis loops.

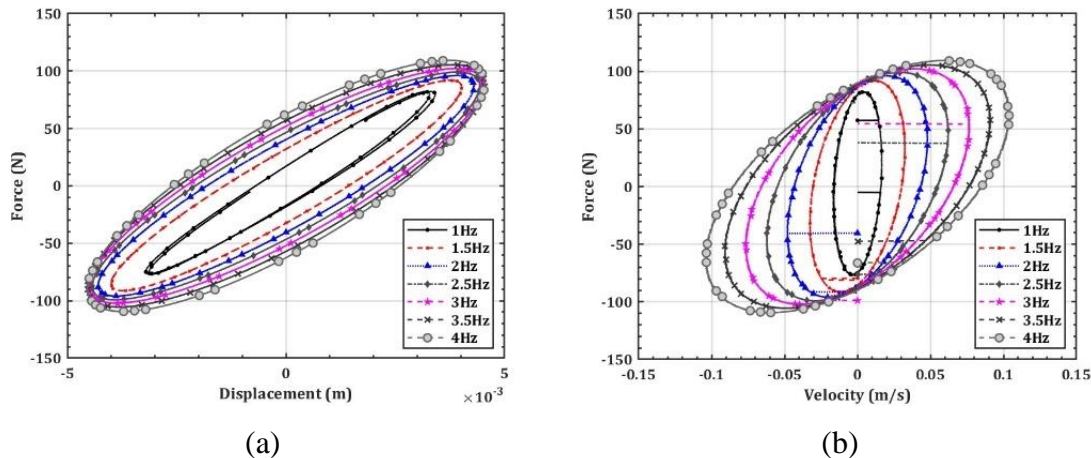


Figure 5 Hysteresis Loops of the PCAD device subjected to Cyclic Displacement Loading Protocol with Variable Frequencies under External Pressure of 1.0 bar (a) Force vs Displacement and (b) Force vs Velocity

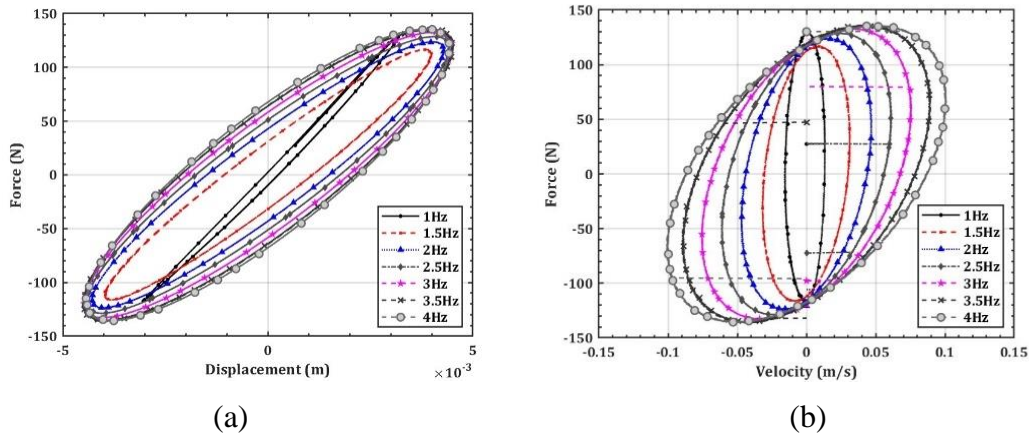


Figure 6 Hysteresis Loops of the PCAD device subjected to Cyclic Displacement Loading Protocol with Variable Frequencies under External Pressure of 1.5 bar (a) Force vs Displacement and (b) Force vs Velocity

To study the effect of external pressure on PCAD device, damper force-displacement and damper force-velocity are plotted for representative cyclic displacement input frequencies 1 Hz and 3 Hz in Fig. 7 (a) and Fig. 7 (b) and Fig. 8 (a) and Fig. 8 (b), respectively. It is evident from these Figures that the damper force-displacement relationship established an increase in the stiffness of the PCAD with an increase in external pressure from 1.0 bar to 1.5 bar. Improvement in damping characteristics in PCAD with an increase in external pressure from 1.0 bar to 1.5 bar is demonstrated through the force-velocity relationship since the enclosed area of the hysteresis loop increases, which indicates more energy dissipation under one cycle of input displacement. Fig. 8 (a) and Fig. 8 (b) show similar observations when damper force-displacement and damper force-velocity relationship are shown for PCAD subjected to cyclic displacement input of 3 Hz frequency under external pressure of 1.0 bar and 1.5 bar. It is important to note that with an increase in external pressure on PCAD stiffness offered tends to increase substantially. However, the width of hysteresis loops shows a reduction for lower frequencies of cyclic input to PCAD, due to pressurized air, which offers resistance. Various parameters, peak displacement, peak damper force, stiffness and area of hysteresis loop for each cyclic displacement frequency subjected to external pressure of 1.0 bar and 1.5 bar were evaluated from the force-displacement relationship shown in Fig. 7 (a) and Fig. 8 (a).

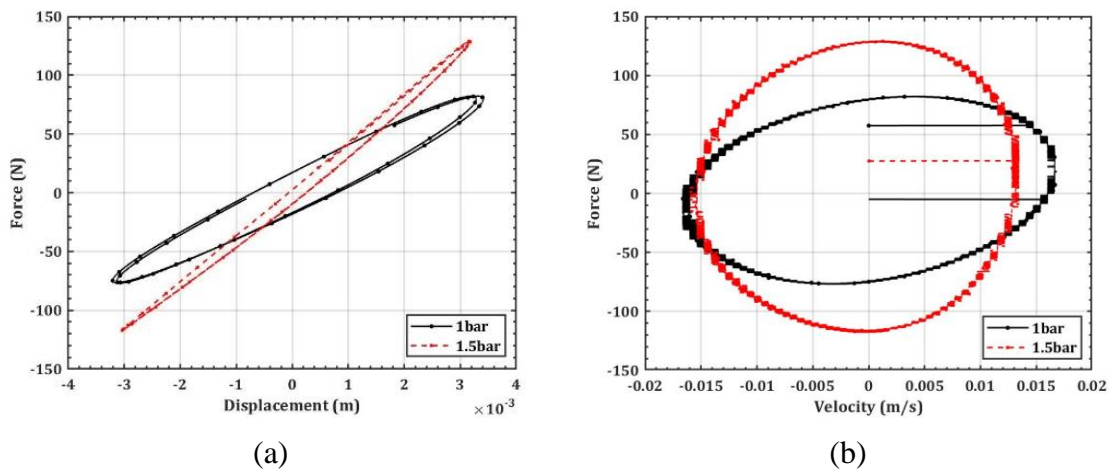


Figure 7 Hysteresis Loops of the PCAD device subjected to Variable External Pressure with Cyclic Displacement Loading Protocol of 1 Hz Frequency (a) Force vs Displacement and (b) Force vs Velocity

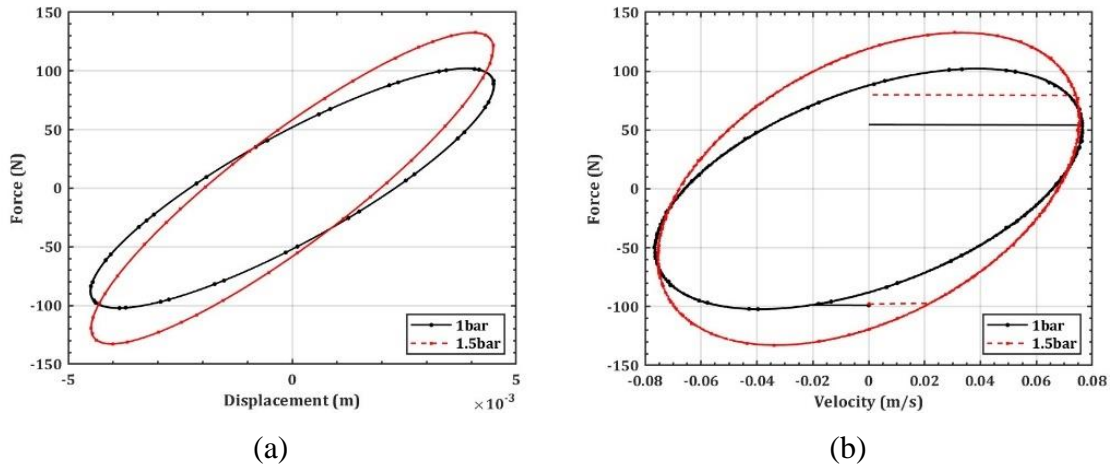


Figure 8 Hysteresis Loops of the PCAD device subjected to Variable External Pressure with Cyclic Displacement Loading Protocol of 3 Hz Frequency (a) Force vs Displacement and (b) Force vs Velocity

Table 1 summarises these parameters for PCAD subjected to varying displacement input under constant external pressure of 1.0 bar. It is evident that damper force was found to increase with the increase in frequency of cyclic displacement loading. The amount of damper force produced by the PCAD ranges between ~80 N to ~109 N, and thus, a full-scale development of PCAD devices with larger dimensions can be developed to produce damper force of large magnitude suitable for the full-scale building model. It can be realized that the stiffness offered by the PCAD was found to be of the same order across various displacement input frequencies. However, the enclosed area of the hysteresis loop tends to increase with input frequencies, indicating improvement in the damping characteristics.

Table 1 Characterization Parameters for Hysteresis behavior of the PCAD subjected to Cyclic Displacement Loading Protocol with Variable Frequencies under External Pressure of 1.0 Bar

Loading Frequency (Hz)	Area of Hysteresis Loop (N-m)	Peak Displacement (m)		Damper Force (N)		Effective Stiffness K_{eff} (N/m)
		Maximum	Minimum	Maximum	Minimum	
1.00	0.28	0.003	-0.003	82.09	-76.77	23995.57
1.50	1.23	0.004	-0.004	92.01	-91.33	22836.44
2.00	2.41	0.004	-0.004	96.09	-95.98	22313.25
2.50	3.20	0.004	-0.004	99.16	-99.16	22364.46
3.00	4.42	0.005	-0.005	102.25	-102.27	22674.42
3.50	6.15	0.005	-0.005	105.63	-105.62	23192.16
4.00	7.58	0.005	-0.005	109.39	-109.39	24058.08

Parameters summarized in Table 1 for PCAD subjected to 1.0 bar of external pressure were evaluated for external pressure of 1.5 bar and are repeated in Table 2. It is evident that damper force increases substantially (range 24.43% to 53%) with an increase in external pressure. The damper force produced ranges between ~116 N to 136 N. This is attributed to the increase in stiffness offered by PCAD, which shows a substantial increase. Enclosed area of the hysteresis loop shows an increase, similar to Table 1, with an increase in dynamic input frequencies. This ensures that the PCAD further improves damping characteristics with an increase in the external pressure.

Table 2 Characterization Parameters for Hysteresis behavior of the PCAD subjected to Cyclic Displacement Loading Protocol with Variable Frequencies under External Pressure of 1.0 Bar

Loading Frequency (Hz)	Area of Hysteresis Loop (N-m)	Peak Displacement (m)		Damper Force (N)		Effective Stiffness K_{eff} (N/m)
		Maximum	Minimum	Maximum	Minimum	
1.00	0.28	0.003	-0.003	128.90	-117.52	39541.43
1.50	1.13	0.004	-0.004	116.69	-116.26	29186.22
2.00	2.31	0.004	-0.004	123.79	-123.77	28844.45
2.50	3.49	0.004	-0.004	128.64	-128.76	29111.66
3.00	4.95	0.004	-0.004	132.73	-132.79	29554.93
3.50	6.87	0.005	-0.005	136.11	-136.16	30119.14
4.00	7.79	0.004	-0.004	135.73	-135.74	30578.24

4.1. Equivalent Viscous Damping Coefficient, ζ

Energy dissipation capabilities of damper play an important role in reducing seismic structural response control of the building in which it is fitted. The most simplest form of damping characteristic is viscous damping, which depends on the velocity of the input motion. For most damping devices exhibiting hysteresis behaviour, an equivalent viscous damping coefficient, ζ , defined by Equation (1), is determined by equating the area of the hysteresis loop of one cycle of displacement input with an area of elliptical force-displacement loop in one cycle by linear viscous damper [16].

$$\zeta = \frac{E_d}{2\pi K_{eff} D^2} \quad (1)$$

where,

E_d = Energy dissipated enclosed area of the hysteresis loop of the PCAD representing Energy dissipated in one Cycle of displacement input;

D = Maximum displacement of the PCAD

K_{eff} = equivalent/effective stiffness of the PCAD.

The equivalent/elastic stiffness of the damper can be evaluated from absolute peak displacement and peak damper force observed by the hysteresis loop of the PCAD, given by Equation (2).

$$K_{eff} = \frac{|P_{max}| + |P_{min}|}{|D_{max}| + |D_{min}|} \quad (2)$$

Where, P_{max} is the maximum damper force for compression loading-unloading protocol; P_{min} is the maximum damper force for tension loading-unloading protocol; D_{max} is the displacement associated with P_{max} and D_{min} is the displacement associated with P_{min} .

Equivalent/effective stiffness for the PCAD was calculated under each displacement input with constant external pressure of 1.0 bar and 1.5 bar using Equation (2) and were summarized in Table 1 and Table 2, respectively. Equivalent viscous damping coefficient, ζ , was determined for the PCAD under varying displacement input loading protocol using Equation (1). Fig. 9 depicts the damping coefficient and plotted against displacement input frequencies for the PCAD under constant external pressure of 1.0 bar and 1.5 bar. It can be observed that the value of the damping coefficient, ζ , increases with an increase in the displacement input frequency applied to the PCAD under external pressures.

In fact, the PCAD, which behaves as an under-damped system up to displacement input frequency 2.5 Hz, becomes an overdamped system beyond it under 1.0 bar external pressure. Under external pressure of 1.5 bar, the PCAD becomes an overdamped system beyond the displacement input frequency of 2.0 Hz. Thus, it is realized that the PCAD works well up to a displacement input frequency of 2.5 Hz for an external pressure of 1.0 bar and up to 2.0 Hz for 1.5 bar external pressure. It can be seen that the equivalent viscous damping coefficient, ζ , tends to decrease for the PCAD with the increase in the external pressure of 1.0 bar to 1.5 bar. This is attributed to limited piston movement inside the pneumatic damper of the PCAD under the influence of higher air pressure of the air chamber and thus, decreasing shearing of air within the air chamber. It should be noted that though energy dissipation capability increases as evident for higher enclosed areas of the hysteresis loop of force-displacement, equivalent viscous damping coefficient, ζ , tends to decrease for the PCAD under 1.5 bar external pressure since equivalent/effective stiffness increase vis-à-vis external pressure of 1.0 bar.

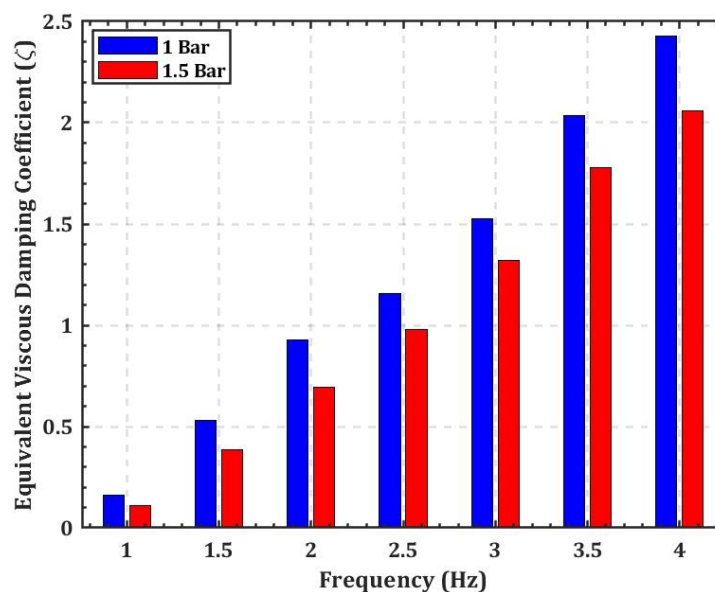


Figure 9 Equivalent Viscous Damping Coefficient for the Prototype PCAD Device subjected to Cyclic Displacement Loading Protocol with Variable Frequencies and External Pressure of 1.0 Bar and 1.5 Bar

5. CONCLUSIONS

Seismic structural response control can be achieved by a variety of seismic protection systems developed over the years. Out of these, supplemental damping devices like; passive damper, active damper, and semi-active damper installed with building system have been found effective and, thus, widely adopted. Passive damper, owing to its robustness, stability over a wide frequency range and easy to maintain, are more attractive and preferred against active and semi-active dampers. The present study aims to develop a prototype Passive Controlled air damper (PCAD), a passive damping device, as a low-cost technological solution to be implemented with the building system. A piston-based pneumatic cylinder with an accumulator was used to fill with air with external pressure applied from an air compressor and regulated by Filter-Regulator-Lubricator (FRL).

A prototype PCAD device was subjected to a cyclic dynamic input loading protocol of varying frequencies under constant displacement amplitude with two external pressure levels of 1.0 bar and 1.5 bar. Hysteresis behaviour of the PCAD was studied through damper force-displacement and damper force-velocity relationships.

It was established that PCAD yields a stable hysteresis loop under varying cyclic displacement input, ensuring energy dissipating capacity of the damper. It was observed that the damper force increases with an increase in cyclic displacement input as well as with an increase in the external pressure. The damping characteristics of the PCAD were studied, defining equivalent viscous damping coefficient, ζ , for varying displacement input frequencies and external pressure inputs of 1.0 bar and 1.5 bar. It was seen that the damping coefficient, ζ , increases with an increase in the displacement input frequency, but decreases with an increase in external pressure to the PCAD. It was found that the PCAD device works well with lower frequencies of displacement input since higher frequencies of input motion convert the damper into an overdamped system.

REFERENCES

- [1] S. K. Jain, "Earthquake safety in India: achievements, challenges and opportunities," *Bull. Earthq. Eng.*, vol. 14, no. 5, pp. 1337–1436, May 2016
- [2] M. H. El Ouni, M. Abdeddaim, S. Elias, and N. Ben Kahla, "Review of Vibration Control Strategies of High-Rise Buildings," *Sensors*, vol. 22, no. 21. MDPI, Nov. 01, 2022
- [3] B. G. W Housner *et al.*, "Structural control: past, present, and future," *J. Eng. Mech.*, vol. 123, pp. 897–971, 1997
- [4] B. F. Spencer and M. K. Sain, "Controlling buildings: a new frontier in feedback," *IEEE Control Syst. Mag.*, vol. 17, no. 6, pp. 19–35, 1997
- [5] T. T. Soong and A. M. Reinhorn, "An Overview of Active and Hybrid Structural Control Research in the U.S.," 1993
- [6] T. T. Soong and B. F. Spencer, "Supplemental energy dissipation: state-of-the-art and state-of-the-practice," *Eng. Struct.*, vol. 24, no. 3, pp. 243–259, 2002
- [7] H. Li and L. Huo, "Advances in structural control in civil engineering in China," *Math. Probl. Eng.*, vol. 2010
- [8] A. M. Head, "SAMCO Final Report 2006 F11 Selected Papers: Modern Seismic Protection Systems for Civil and Industrial Structures," 2006
- [9] J. Cao, X. Zhu, F. Li, and X. Jin, "Modeling and Constrained Optimal Design of an Ultra-Low-Friction Pneumatic Cylinder With Air Bearing," *Adv. Mech. Eng.*, 2019
- [10] R. Faraj, C. Graczykowski, and J. Holnicki-Szulc, "Adaptable pneumatic shock absorber," *JVC/Journal Vib. Control*, vol. 25, no. 3, pp. 711–721, 2019
- [11] X. Zhu, X. Jing, and C. Li, "A Magnetorheological Fluid Embedded Pneumatic Vibration Isolator Allowing Independently Adjustable Stiffness and Damping," *Smart Mater. Struct.*, 2011
- [12] A. J. Nieto, A. L. Morales, A. M. González, J. M. Chicharro, and P. Pintado, "An Analytical Model of Pneumatic Suspensions Based on an Experimental Characterization," *J. Sound Vib.*, 2008

- [13] A. de M. Wahrhaftig, C. M. Menezes, R. O. da S. Conceição, I. G. de Oliveira, and O. Ozdemir, “Assessment of a hydraulic bottle jack as an effective device for controlling vibration and mitigating the effects of earthquakes,” *J. Low Freq. Noise Vib. Act. Control*, vol. 43, no. 1, pp. 543–559, 2024
- [14] B. Suci, “Experimental Investigation on a Controllable Colloidal Damper for Vehicle Suspension,” *Mech. Eng. J.*, 2015
- [15] R. Zalewski and P. Bartkowski, “Prototype of a controllable damper based on granular materials subjected to partial vacuum,” *MATEC Web Conf.*, vol. 254, p. 05009, 2019
- [16] Anil Chopra, *Dynamics of structures*. Pearson Education, Inc, 2012

Citation: Utsav K. Koshti and Sharadkumar Purohit, Dynamic Testing of Prototype Pressure Controlled Air Damper Under Cyclic Loading Protocol, *International Journal of Civil Engineering and Technology (IJCIET)*, 15(2), 2024, pp. 1-12.

Abstract Link: https://iaeme.com/Home/article_id/IJCIET_15_02_001

Article Link:

https://iaeme.com/MasterAdmin/Journal_uploads/IJCIET/VOLUME_15_ISSUE_2/IJCIET_15_02_001.pdf

Copyright: © 2024 Authors. This is an open-access article distributed under the terms of the Creative Commons Attribution License, which permits unrestricted use, distribution, and reproduction in any medium, provided the original author and source are credited.

This work is licensed under a **Creative Commons Attribution 4.0 International License (CC BY 4.0)**.



✉ editor@iaeme.com